Adaptive Neuro-Fuzzy Inference System for Echoes Classification in Radar Images

Leila Sadouki[1,2] and Boualem Haddad[2]
[1]*Institute of Electrical and Electronic Engineering, University M'Hamed Bougara of Boumerdes (UMBB), Independence Avenue, 35000 Boumerdes, Algeria*
[2]*Laboratory of Image Processing and Radiation, Faculty of Computer Science and Electronics (USTHB), PObox 32 El Alia. Bab Ezzouar, Algiers, Algeria*

Keywords: ANFIS, Image, Radar, Precipitations, Clutter.

Abstract: In order to remove the undesirable clutter which reduces the radar performances and causes significant errors in the rainfall estimation, we implemented in this paper an algorithm deals with the classification of radar echoes. The radar images studied are those recorded in Sétif (Algeria) every 15 minutes, we used a combination of textural approach, with the grey-level co-occurrence matrices, and a grid partition based fuzzy inference system, named ANFIS-GRID. We have used two parameters, namely Energy and local homogeneity that are considered to be the most effective in discriminating between precipitation echoes and clutter. Those parameters are used as inputs for the ANFIS-GRID, while the output of this system is the radar echo types. In function of the best mean rate of correct recognition and using two different optimization methods, the structure with 2 inputs, 4 membership functions, 16 rules and 1 output was selected as the most efficient ANFIS-GRID. This method gives a mean rate of correct recognition of echoes to over 93.52% (91.30% for precipitation echoes and 95.60% for clutter). In addition, the proposed approach gives a process maximum time of less than 90 seconds, which allows the filtering of the images in real time.

1 INTRODUCTION

The demands for finer scale meteorological services have more and more required higher resolution observations to initialize and evaluate weather and climate models, applications, and products. In response to these demands smart techniques are increasingly used in the design, classification, modeling and control of complex systems, such as neural networks, fuzzy logic and genetic algorithms…

For weather radar, the presence of echoes coming from the earth's surface, or clutter, mixed with precipitation echoes, making the hydrological measurement very difficult (Sauvageot and Despaux, 1990), a good way to eliminate clutter is to compare the statistical properties of the ground echoes to those of precipitations echoes, such as textural features (Haddad et al., 2004). The most common techniques used are Doppler filtering (Doviak and Zrnic, 1993), or dual polarization filtering (Islam et al., 2012; Chandrasekar et al., 2013). Clutter can be removed by analyzing in real time the coefficient of the autocorrelation function of the radar signal (Hamuzu and Wakabayashi, 1991). Others applied the fuzzy logic technique, to classify the Doppler radar echoes types (Hubbert et al., 2009) or for identifying non-precipitating echoes in radar scans (Berenguer et al., 2006; Cho et al., 2006). In (Sadouki and Haddad, 2013), they combined the textural properties of the echoes with the fuzzy approach in order de classify the echoes. Furthermore, (Xiang, 2010) used the neuro-fuzzy approach to eliminate noise in Doppler radar signals.

Depending on the on above literature survey, it's interesting to implement an algorithm which combines the textural features, based on the method of grey-level co-occurrence matrices, and an Adaptive Neuro-Fuzzy System (ANFIS) with grid partition. The input variables for our system are two textural parameters considered as effective elements for distinguishing between precipitation echoes and clutter (Sadouki and Haddad, 2013). This method was applied to the images taken in the region of Sétif (Algeria).

Sadouki, L. and Haddad, B.
Adaptive Neuro-Fuzzy Inference System for Echoes Classification in Radar Images.
DOI: 10.5220/0005717401590166
In *Proceedings of the 11th Joint Conference on Computer Vision, Imaging and Computer Graphics Theory and Applications (VISIGRAPP 2016) - Volume 4: VISAPP*, pages 159-166
ISBN: 978-989-758-175-5

The remainder of the paper is organized as follows: Section 2 focuses on database used in this work, sections 3 and 4 deal respectively with the used concepts and the data processing. We illustrate discuss and validate the different results in sections 5 and 6. Finally, and in section 7, we give our conclusion.

2 DATA BASE

Weather radar of Sétif is of the Type AWSR-81 (Algerian Weather Service Radar). It is non-coherent pulsed radar which consists of a transmitter, a receiver, a duplexer, antenna of 3 m in diameter and is associated with a SANAGA chain (Système d'Acquisition Numérique pour l'Analyse des Grains Africains) which is a system of acquisition and digitization of images (Sauvageot and Despaux, 1990). The main characteristics of this radar are:

- Transmission power: 250 kW;
- Transmission frequency: 5.6 GHz;
- Reception sensitivity to: -110 dBm;
- Pulse width: 2µs;
- Antenna gain: 30 dB;
- Return period: 4 ms;
- Beam width (3 dB): 1.1;

Our database consists of images taken during the period of 1997-2001. Sétif radar is positioned at latitude of 36°11'N, a longitude of 5°25' E and an altitude of 1700 m above the sea level. It records every fifteen minutes an image of 512×512 pixels using the PPI (Plan Position Indicator) presentation, with a resolution of 1 km per pixel.

As shown in the image of Figure 1, the images recorded in this site using the C-band meteorological radar, use a palette of sixteen colors. We find in those images a lot of ground echoes coming from the earth's surface. These echoes are, in particular, due to the fact that Sétif region is a part of the Algerian highlands and its Radar is surrounded by several ground obstacles. The nearest ground echoes are produced largely by the industrial area. Beyond the horizon, the ground obstacles produce several ground echoes in the radar images. For example, to the southwest, 60 km away from the radar, there are the mountains of Djurdjura, which reach an altitude of 2300 m. In the same direction, 40 km away from the radar, we find the mountains of Bibans with a height of 1417 m. To the northeast, at a shorter distance (about 30 km away from the radar), are located the mountains of Babors, which reach an altitude of 2004 m.

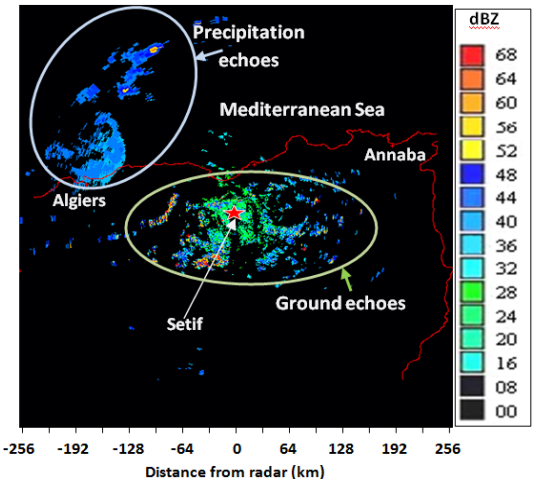

Figure 1: Radar images of Sétif.

3 USED CONCEPTS

The main methods that are considered in this paper are textural approach, using the co-occurrence matrices, and the Neuro-Fuzzy controller. The latter, is the combination of the Neural networks and Fuzzy logic, that takes advantages of both approaches. Figure 2 summarizes the concepts used in this study.

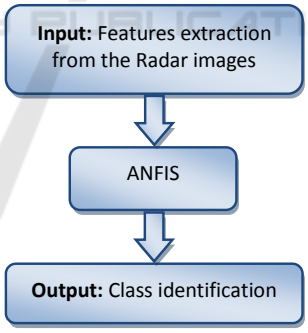

Figure 2: Block diagram of the used concepts.

3.1 Co-occurrence Matrices

The grey-level co-occurrence matrices are among the most frequently used statistical methods in the field of the texture analysis of the radar and the satellite images (Haralick, 1979). The gray-level Co-occurrence matrix of an image is obtained by estimating the joint conditional density of probability functions of second-order P (i, j / d, θ), the latter represents the transition probability of a pixel of gray level "i" to a pixel of gray level "j".

This transition is controlled by: the distance "d" between the two pixels and the orientation "θ"which is defined by the angle between the direction of transition and the image scanning direction.

The orientation "θ" can be determined also with Cartesian coordinates (Δx, displacement in the horizontal direction and Δy, displacement in the vertical direction)

The elements P (i, j) denoted Pij of the Co-occurrence matrix represent the frequency of occurrence of the pair of gray levels (i, j) in the processing window "W" of T1×T2 size, according to a relationship represented by the pair (Δx, Δy). They are defined as follows:

$$P(i, j/\Delta x, \Delta y) = \text{Card}\{(m, n), (m+\Delta x, n+\Delta y) \in W / I(m, n) = i \text{ and } I(m+\Delta x, n+\Delta y) = j\} \quad (1)$$

Where Card, is the cardinal or the number of elements, and I (m, n) and I (m+Δx, n+Δy) represent respectively the intensities of pixels "i" and "j" located at (m,n) and (m+Δx, n+Δy) in the window "W".

The elements of the direction matrix C_{ij} (θ, d) are written:

$$C_{ij}(\theta, d) = P(i, j / \Delta x, \Delta y) / r \quad (2)$$

Where "r" is the normalization parameter which is equal to: (T1-|Δx|) × (T2-|Δy|).

There are eight Co-occurrence matrices C (θ, d) for different directions (θ = 0°, 45°, 90°, 135°, 180°, 225°, 270°, 315°).

We can calculate, using the Co-occurrence matrix, a set of statistical properties (i.e. Mean, Variance, Inertia, Local homogeneity, Energy, Correlation, Entropy, Nuances grouping, and Predominance grouping), which allow us to reveal the particular characteristics of image texture. In this paper, we will use only two parameters (i.e. Local homogeneity and Energy) that give the results the most uncorrelated, with the direction θ =0° and the distance d=1, which correspond to the Cartesian coordinates (Δx=0, Δy=1) (Sadouki and Haddad, 2013).

It's worth noting that, among the values of d= {1,2,3,4}, the distance d = 1, was chosen, by experience, as the best value in terms of effectiveness (in distinguishing between precipitation echoes and clutter) and the proportionality with the size of the study windows (5×5 pixels window).

Equations of those parameters are: (Haralick, 1979; Unser, 1986; Peckinpaugh, 1991).

- Energy which measures textural uniformity:

$$E = \sum_{i=0}^{N_g-1} \sum_{j=0}^{N_g-1} C_{ij}^2 \quad (3)$$

- The local homogeneity that gives greater weight to the occurrence frequencies of homogeneous zones:

$$H_L = \sum_{i=0}^{N_g-1} \sum_{j=0}^{N_g-1} \left[C_{ij} / \left(1 + (i-j)^2\right) \right] \quad (4)$$

3.2 Neuro-Fuzzy Concept

A Neuro-Fuzzy (NF) system is a combination of Artificial Neural Network (ANN) and Fuzzy Inference System (FIS) in such a way that ANN learning algorithms are used to determine the parameters of FIS (Kurian et al., 2006).

ANFIS (Adaptive Neuro-Fuzzy Interface System) is the fuzzy Sugeno model based paradigm that grasps the learning abilities of ANN to enhance the intelligent system's performance using a priori Knowledge.

Using a given input/output data set, ANFIS constructs a fuzzy inference system (FIS) whose membership function parameters are tuned using either a back-propagation algorithm alone, or in combination with a least squares method. This allows your fuzzy systems to learn from the data they are modeling. The learning method works similarly to that of neural networks (Chaudhari et al., 2012). In fact, ANFIS cancels out the interference and gives better performance even if the complexity of the signal is very high.

We used in this paper, the ANFIS-GRID fuzzy inference system which is the combination of grid partition and ANFIS. Grid partition divides the data space into rectangular sub-spaces using axis-paralleled partition based on predefined number of membership functions and their types in each dimension as shown in Figure 3.

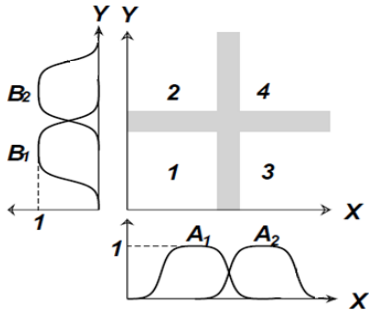

Figure 3: Grid partition of an input domain with 2 input variables and 2 membership functions for each input.

The number of fuzzy rules increases exponentially when the number of input variables increases. For example, if there are averagely "m" membership functions (MF) for every input variable and a total of "n" input variables for the problem, the total number of fuzzy rules is "m^n" (Wei et al., 2007).

For a first-order Sugeno fuzzy model, a common rule set with "k" fuzzy "if-then" rules is given by: (Bhavani et al., 2012)

Rule k:

```
If X is Ai and Y is Bj,
Then fk = pk X + qk Y + rk
```

Where: k=1...i*j

To present the ANFIS architecture, let us consider the example of the Figure 4 which has two inputs (X , Y), and one output "f".

Layer 1: Calculate Membership Value for Premise Parameter: Every node "i" in this layer is an adaptive node

Layer 2: Firing strength of rule: The nodes in this layer are fixed (not adaptive).These are labeled "Π" to indicate that they play the role of a simple multiplier.

Layer 3: Normalize firing strength: Nodes in this layer are also fixed nodes. These are labeled "N" to indicate that these perform a normalization of the firing strength from previous layer.

Layer 4: Consequent Parameters: All the nodes in this layer are adaptive nodes.

Layer 5: Overall output: This layer has only one node labeled "**Σ**" indicated that is performs the function of a simple summer.

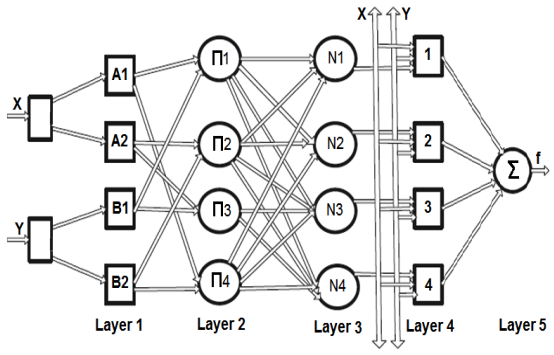

Figure 4: ANFIS Architecture (an example with 2 inputs and 4 rules).

4 DATA PROCESSING

To classify the types of echoes in radar images, a variety of samples (sub-image), carefully selected from images, where precipitation echoes (class 1) are distinctly separated from the ground echoes (class 2). It's important to note that each sub-image, of a maximum size of about 15×15 pixels, illustrates a different meteorological situation.

For each 5×5 pixels window in a given sub-image, we calculated the statistical parameters Energy and Local homogeneity that have been found to be useful in discriminating between precipitations and clutter, and have been chosen as inputs of our classifier. (Sadouki and Haddad, 2013)

As result to the previous process, we were capable to construct our database of 1000 vectors that corresponds to our two classes, 500 for clutter and 500 for precipitations. Each vector is composed of 3 elements, Energy, Local homogeneity and class.

In fact, we used MATLAB commands for learning process with 1000 epochs and 600 training sample from the two classes. In addition, the optimization methods applied, in order to train the membership function's parameters to emulate the training data, are the back-propagation and the hybrid methods, where the second method is a combination of least-squares and back-propagation gradient descent method.

It's worth mentioning that the others 400 vectors of our data base were use in the testing process.

The output of the ANFIS classifier will be used later to find an appropriate approach, which will allow us to separate the ground echoes from the precipitation echoes in order to eliminate the undesirable echoes.

5 RESULTS AND DISCUSSION

After creating different architectures of ANFIS classifier, and using triangular membership functions for each Input, we perform the training of each classifier using our database. Since the errors, obtained during training and testing, seem to be of the same level, so, we were obliged to validate our classifier. Thus, we classified 20 images using 8 different topologies, after that, we calculated the rate of correct recognition for each image (denoted RCR). This rate is calculated by the following expression:

$$RCR = \left(\sum_{i=1}^{c} X_i / N\right) \times 100 \quad (5)$$

Where:
c : Is the number of classes.
N : Is the total number of pixels.
Xi : Is the number of pixels correctly classified to the class i.

Table 1 collects the results obtained, with different topologies and by changing:

- The number of Membership Functions for each input (MFin1-MFin2),
- Rules.
- Optimization Method.

Where, MFin1 and MFin2 are the number of membership functions for the parameters Energy and local homogeneity respectively.

Table 1: Rate of correct recognition (RCR in %) and the associated time (in Seconds) for different topologies and different optimization methods (average of 20 images).

Topology (MFin1-MFin2)	Back propagation Opt. Method		Hybrid Opt. Method	
	RCR	Time	RCR	Time
(2-2)	92,85	71.30	92,65	72.14
(3-3)	92,96	71.61	92,22	73.13
(4-4)	93,52	72.14	92,57	74.93
(5-5)	90,60	73.25	91,95	75.78
(6-6)	83,89	73.78	92,30	76.70
(7-7)	79,42	74.84	92,88	77.19
(10-10)	75,37	76.28	88,52	80.40
(15-15)	73,11	78.67	87,16	81.23

According to the results of the Table 1, it's clear that from the topology (5-5) and when we use the back propagation method, the RCR decreases with the increasing of the number of the membership functions, but for the hybrid method, the same rate decreases from the level (7-7). Also, we can see that the most adequate topology, which was fixed after several trials based on the best rate of correct recognition, is the (4-4) network with the back propagation optimization method, with 2 inputs, 4 membership functions, 16 rules and 1 output. In addition the processing time is less than 90 seconds, which is a relatively small time comparing with the image acquisition time.

The model of this ANFIS is shown in Figure 5.

Rules:

- Rules 1 to 4: with i,j=1..4
  If (Input1 is In1MF1) and (Input2 is In2MFi) then (Output is OutMFj)
- Rules 5 to 8: with i=1..4 and j=5..8
  If (Input1 is In1MF2) and (Input2 is In2MFi) then (Output is OutMFj)
- Rules 9 to 12: with i=1..4 and j=9..12
  If (Input1 is In1MF3) and (Input2 is In2MFi) then (Output is OutMFj)
- Rules 13 to 16: with i=1..4 and j=13..16
  If (Input1 is In1MF4) and (Input2 is In2MFi) then (Output is OutMFj)

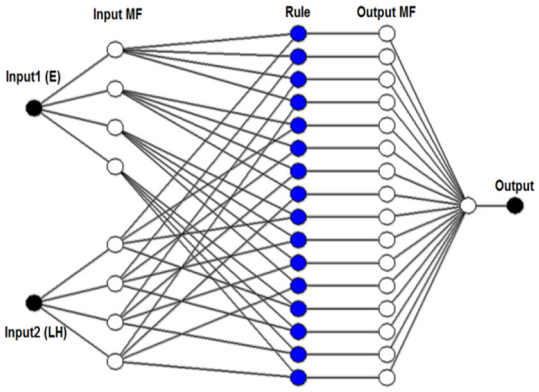

Figure 5: ANFIS Structure.

Where, OutMFj (j=1..16) are the membership functions of the outputs.

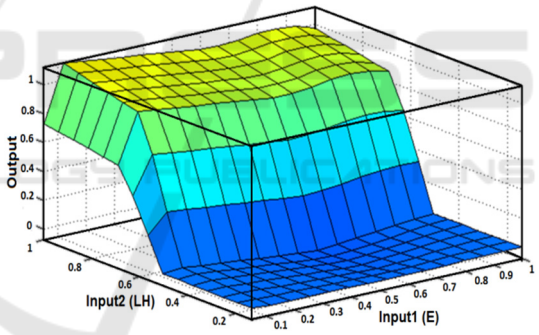

Figure 6: ANFIS Surface View.

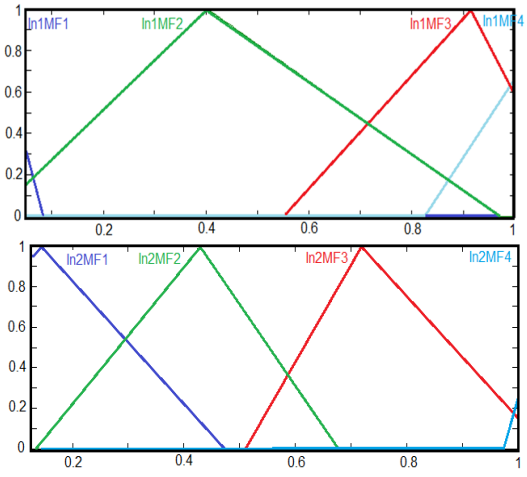

Figure 7: Membership functions plot (final forms).

The ANFIS surface view and the final forms of the 4 membership functions of each input are shown in Figure 6 and Figure 7 respectively. Where, In1MFi (i=1..4) are the membership functions of the first input Energy or "E", while In2MFi are the membership functions of the second input Local Homogeneity or "HL".

As illustration of the output of our classifier, the image of Figure 8 recorded in 09 November 2001 is considered. It provides the case were the precipitations partially cover the ground echoes.

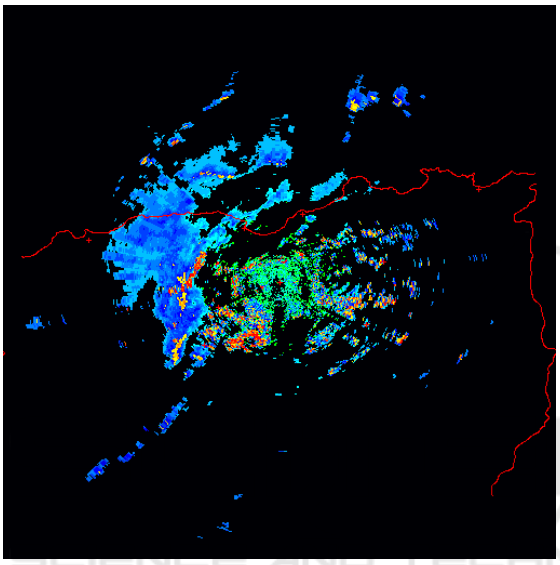

Figure 8: Radar image of Sétif region recorded in 09/11/2001.

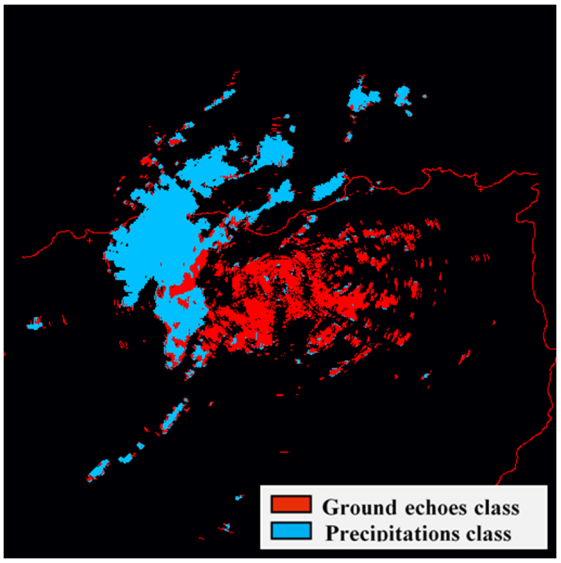

Figure 9: Radar image of Sétif region (Classified image).

In order to eliminate the undesirable echoes or clutter, we used our approach, to classify and filter this image with the (4-4) ANFIS network. To do that, we performed the following process:

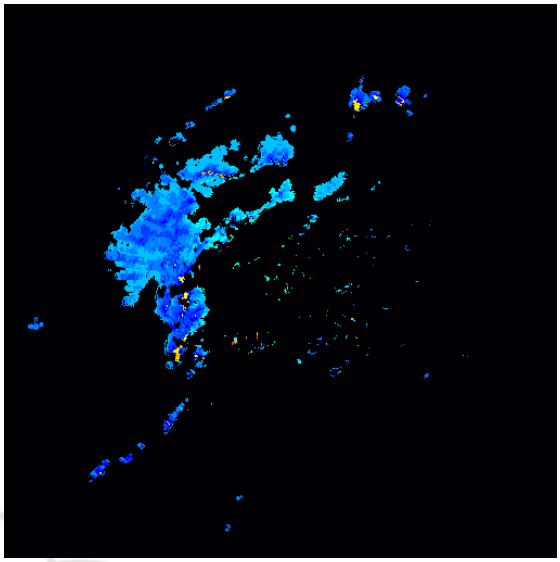

Figure 10: Radar image of Sétif region (Filtered image).

For each pixel in the image and using the surrounded pixels, we computed the parameters Energy and Local homogeneity, after that, we applied them to the ANFIS network to get, as result, the appropriate class for that pixel. With this classifier, we can observe clearly through Figure 9 that the two classes are well classified.

Whereas for the filtering, and for each pixel in the image, we performed the following test: If the current pixel is evaluated in the class of clutter, we assign the black colour for that pixel, otherwise, we maintain the initial colour. Figure 10 shows that the ground echoes appearing on the considered image of Sétif are eliminated and the precipitation fields are a little bit affected by the filtering.

6 VALIDATION

It's very important to note that for the case of images, where the precipitations cover partially the ground echoes, the estimations of the RCR in the images, are very difficult. Consequently, we were obliged to use another way to validate our technique, which is the estimation of the intensity of rainfall using the radar relationship for temperate climates: (Sauvageot, 1992)

$$Z = 300\ R^{1.5} \quad (6)$$

Where Z and R are, respectively, the radar reflectivity factor (expressed in $mm^6\ m^{-3}$) and the precipitation rate (expressed in mm h^{-1}).

To verify that the filtering of clutter does not affect the reflectivity of precipitation echoes, we compared the intensity of rainfall collected and measured by pluviometer, and that estimated by radar images during the extreme rain event, observed on November 09-10, 2001 in the region of Algiers, which was at the origin of a natural disaster.

We recorded in the day of November 10th an amount of rain equals to 132 mm in 6 hours duration (6:00 to 12:00). (Haddad et al., 2003)

Since we have a chronological set of 25 images recorded from 6:00 am to 12:00 pm, we were capable to find the intensity of rainfall estimated by the filtered radar images which is 121.6 mm. Thus, the estimation error is about 7.87%.

7 CONCLUSIONS

The method described in this paper shows that the combination of the textural features, using Co-occurrence matrices, and Adaptive Neuro-Fuzzy Interface System, with the utilization of grid partition, allows an efficient radar echoes classification. In function of two factors which are filtering rate and computation time, the structure 2 inputs with 4 membership functions for each and 16 (or 4^2) rules was selected as the most efficient network. The application of this approach gives a mean rate of correct recognition of echoes to over 93.52% (91.30% for precipitation echoes and 95.60% for clutter) for the images recorded in the site of Sétif. In addition, time of processing is about 90s which is less than 2 minutes. It would be interesting to extend this study to other sites of different climates to check the effectiveness of the technique and if the thresholds and membership functions always stay invariant.

ACKNOWLEDGEMENTS

The authors would like to thank the National Meteorology Office of Algeria for providing the radar data base used in this study. We would also like to thank the reviewers for their valuable comments and suggestions.

REFERENCES

Berenguer, M., Sempere-Torres, D., Corral, C. and Sanchez-Diezma, R., 2006. A fuzzy logic technique for identifying nonprecipitating echoes in radar scans. *Journal of Atmospheric and Oceanic Technology*, vol. 23, pp. 1157-1180.

Bhavani Sankar, A., Kumar, D., and Seethalakshmi, K., 2012. A New Self-Adaptive Neuro Fuzzy Inference System for the Removal of Non-Linear Artifacts from the Respiratory Signal. *Journal of Computer Science*. vol. 8 (5), 621-631.

Chandrasekar, V., Keränen, R., Lim, S., and Moisseev, D., 2013. Recent advances in classification of observations from dual polarization weather radars. *Atmospheric Research*, vol. 119, pp. 97-111.

Chaudhari, O. K., Khot, P. G., Deshmukh, K. C., and Bawne, N. G., 2012. ANFIS based model in decision making to optimize the profit in farm cultivation. *International Journal of Engineering Science and Technology (IJEST)*. Vol. 4 (2), 442-448.

Cho, Y. H., Lee, G., Kim, K. E. and Zawadzki, I., 2006. Identification and removal of ground echoes and anomalous propagation using the characteristics of radar echoes. *Journal of Atmospheric and Oceanic Technology*. vol. 23, pp. 1206-1222.

Doviak, R. J., and Zrnic, D. S., 1993. *Doppler radar and weather observations*, Academic Press., pp. 562.

Haddad, B., Sadouki, L., Naili, R, Adane, A., and Sauvageot, H., 2003. Analyse De La Dimension Fractale Des Echos De Precipitations: Cas Des Inondations D'Alger. *Publication de l 'Association Internationale de Climatologie*. vol. 15, pp.386-392.

Haddad, B., Adane, A., Sauvageot, H., and Sadouki, L., 2004. Identification and filtering of rainfall and ground radar echoes using textural features. *International Journal of Remote Sensing*. vol. 25(21), pp. 4641–4656.

Hamuzu, K., and Wakabayashi, M., 1991. Ground clutter rejection. In Hydological applications of Weather Radar, *Clukie and Collier. Ed Ellis Horwood Ltd*, pp. 131–142.

Haralick, R. M., 1979. Statistical and structural approaches to textures. *Proceedings of the IEEE on Image Processes*, vol. 67, pp. 786–804.

Hubbert, J. C., Dixon, M., and Ellis, S. M., 2009. Weather Radar Clutter. Part II: Real-Time identification and filtering. *Journal of Atmospheric and Oceanic Technology*, vol. 26, pp. 1181–1197.

Islam, T., Rico-Ramirez, M. A., Han, D. and Srivastava, PK., 2012. Artificial Intelligence Techniques for Clutter Identification with Polarimetric Radar Signatures. *Atmospheric Research*, 109-110, pp. 95-113.

Kurian, C. P., George, V. I., Jayadev, B., and Radhakrishna, S. A., 2006. ANFIS Model For The Time Series Prediction of Interior Daylight illuminance. *AIML Journal*. Vol. 6 (3).

Peckinpaugh, S. H., 1991. An Improved Method for Computing Grey-Level Co-Occurrence Matrix Based

Texture Measures. *CVGIP: Graphical Models and Image Processing*. vol. 53, 574–580.

Sadouki, L., and Haddad, B., 2013. Classification of radar echoes with a textural–fuzzy approach: an application for the removal of ground clutter observed in Sétif (Algeria) and Bordeaux (France) sites. *Int. J. of Remote Sensing*, vol. 34(21), 7447-7463.

Sauvageot, H., and Despaux, G., 1990. SANAGA: Un système d'acquisition numérique et de visualisation des données radar pour la validité des estimations satellitaires de précipitations. *Veille Climatique Satellitaire*, vol. 31, pp. 51–55.

Sauvageot, H., 1992. *Radar Meteorology*. Norwood: Artech House., pp. 361.

Unser, M., 1986. Sum and difference histograms for texture classification. *IEEE Transactions on Pattern Analysis and Machine Intelligence*. vol. 8(1), pp. 118–125.

Wei, M., Bai, B., Sung, A. H., Liu, Q., Wang, J., and Cather, M. E., 2007. Predicting injection profiles using ANFIS. *Information Sciences*. vol. 177, 4445–4461.

Xiang, L., 2010. Adaptive Network Fuzzy Inference System Used in Interference Cancellation of Radar Seeker. *IEEE International Conference on Intelligent Computing and Intelligent Systems (ICIS)*. vol. 2, pp. 93–97.